Journal of Nuclear Medicine, published on October 13, 2016 as doi:10.2967/jnumed.116.178509

Clinical Trial Using Sodium Pertechnetate ^{99m}Tc Produced with Medium-Energy Cyclotron: Biodistribution and Safety Assessment in Patients with Abnormal Thyroid Function

Svetlana V. Selivanova[1,2,*], Éric Lavallée[1], Helena Senta[1], Lyne Caouette[1], Alexander J.B. McEwan[3], Brigitte Guérin[2,1], Roger Lecomte[2,1], Éric Turcotte[1,2]

[1] Sherbrooke Molecular Imaging Center, CRCHUS, Sherbrooke, QC, Canada

[2] Department of Nuclear Medicine and Radiobiology, Faculty of Medicine and Health Sciences, Université de Sherbrooke, Sherbrooke, QC, Canada

[3] Cross Cancer Institute, Edmonton, AB, Canada

*Corresponding author: Svetlana V. Selivanova, CIMS, CRCHUS, 3001, 12th Avenue Nord, Sherbrooke, QC, J1H 5N4, Canada; phone: +1-819-346-1110 ext.16637; fax: +1-819-829-3238; e-mail: Svetlana.V.Selivanova@USherbrooke.ca

Running title: Cyclotron-produced ^{99m}Tc: clinical trial

Word count: 5180

Financial support: Natural Resources Canada through the Isotope Technology Acceleration Program (ITAP), Medical Imaging Trial Network of Canada (MITNEC)

ABSTRACT

A single-site prospective open-label clinical study with cyclotron-produced sodium pertechnetate ^{99m}Tc (^{99m}Tc-$NaTcO_4$, ^{99m}Tc-pertechnetate) was performed in patients with indication for a thyroid scan to demonstrate the clinical safety and diagnostic efficacy of the drug and confirm its equivalence with conventional sodium pertechnetate ^{99m}Tc eluted from a generator. **Methods:** Sodium pertechnetate ^{99m}Tc was produced with a cyclotron (24 MeV, 2 h irradiation) from enriched ^{100}Mo (99.815%) or supplied by a commercial manufacturer (bulk vial eluted from a generator). Eleven patients received 325±29 MBq of the cyclotron-produced ^{99m}Tc-pertechnetate, while their age/sex matched controls received a comparable amount of the generator-derived tracer. Whole-body and thyroid planar images were obtained for each participant. In addition to the standard 140.5 keV ±7.5% energy window, data were also acquired in a lower (117 keV ±10%) and a higher (170 keV ±10%) energy windows. Vital signs, hematological and biochemical parameters were monitored before and after tracer administration. **Results:** Cyclotron-produced ^{99m}Tc-$NaTcO_4$ showed organ and whole-body distribution identical to those of conventional ^{99m}Tc-pertechnetate and was well tolerated. All images lead to a clear final diagnosis. While the number of counts in the higher energy window increased significantly for the cyclotron-produced ^{99m}Tc-$NaTcO_4$, this did not influence image quality in the standard energy window. Image definition in the standard energy window was equivalent and without particular features allowing discrimination between ^{99m}Tc production methods. **Conclusion:** Systemic distribution, clinical safety, and imaging efficacy in humans provide supporting evidence for the use of cyclotron-produced ^{99m}Tc-pertechnetate in routine clinical practice as an equivalent for generator-eluted ^{99m}Tc-$NaTcO_4$.

Keywords: ^{99m}Tc-pertechnetate, cyclotron, thyroid imaging, safety, efficacy

INTRODUCTION

Despite a steady increase in procedures utilizing positron emission tomography (PET), the role of technetium-99m (^{99m}Tc) in nuclear imaging remains important and it will continue to be heavily used in years to come (*1*). At the same time, conventional supply chain of ^{99m}Tc is currently fragile due to aging nuclear reactors and the transition period from the use of highly-enriched uranium to low-enriched uranium in targets for nuclear reactors. In addition, full-cost recovery for production of medical isotopes promises to hike the prices for ^{99}Mo/^{99m}Tc generators, rendering alternative technologies for the production of medical isotopes more competitive (*2*). Direct production of ^{99m}Tc by cyclotrons is a decentralized approach that could satisfy the demand for ^{99m}Tc on a regional level (*3*), and help alleviate ^{99m}Tc under-supply in case of need.

Production of ^{99m}Tc via proton irradiation of enriched ^{100}Mo results in a co-production of several ^{9x}Tc radionuclides. Hence, the safety and imaging characteristics of cyclotron-produced ^{99m}Tc must be assessed for any unanticipated adverse effects. The first clinical trial demonstrated that cyclotron-produced ^{99m}Tc-pertechnetate obtained at 17 MeV was safe in humans (*4*). Theoretical (*5*) and empirical analyses (*6*) showed that the ^{99m}Tc production yield doubles when incident energy increases from 16 MeV to 24 MeV. However, the radionuclidic purity greatly depends on the irradiation conditions, in particular, on the incident proton beam energy and irradiation time (*6*,*7*). To take advantage of the higher production capacity of medium-energy cyclotrons, we first investigated the quality of ^{99m}Tc produced at 24 MeV. Its chemical and radiochemical purity, as well as patient dosimetry, were shown to be suitable for human use (*7*). A prospective open-label clinical study with sodium pertechnetate ^{99m}Tc prepared with a cyclotron at 24 MeV was initiated in patients with a thyroid scan indication to demonstrate

the clinical safety and diagnostic efficacy of the radiopharmaceutical and confirm its utility in clinical procedures (ClinicalTrials.gov identifier: NCT02307175, approved by Health Canada). The images were analyzed qualitatively and quantitatively and compared with those obtained with conventional sodium pertechnetate ^{99m}Tc eluted from a generator. The results of this clinical trial are presented herein.

MATERIALS AND METHODS

Provision of Sodium Pertechnetate ^{99m}Tc

Technetium-99m was produced on site with a TR-24 cyclotron (Advanced Cyclotron Systems, Inc.) by irradiation of enriched ^{100}Mo (99.815%; ^{98}Mo 0.17%, $^{92–97}$Mo each 0.003%) at 24 MeV for 2 h, as described previously (*7*). The targets were processed to recover an effective thickness corresponding to approximately 5-MeV energy loss. Extraction of ^{99m}Tc was performed following a published procedure (*7*) modified from (*8*). Quality control of the formulated sodium pertechnetate ^{99m}Tc solution for injection was done for all prepared batches according to standard procedures described earlier (*7*). The endotoxin levels were assayed using Limulus amebocyte lysate method with Endosafe-PTS test system (Charles River Laboratories International, Inc). Sterility tests were performed by a licensed laboratory (Nucro-Technics, Scarborough, ON). Generator-eluted ^{99m}Tc was supplied by Isologic Innovative Radiopharmaceuticals.

Study Design

A single-site prospective non-randomized case-control open-label study enrolled 19 patients referred to the nuclear medicine department with indication for a thyroid scan. The study was approved by the Institutional Ethics Committee and by Health Canada. Each subject signed an approved written informed consent form. The study recruited a

population of patients with thyroid disease (hyperthyroidism or thyroid nodule assessment), 18−80 years of age, with biochemical parameters within normal limits for the age, and Karnofsky performance status over 50%. Eleven recruited participants were administered with the cyclotron-produced ^{99m}Tc-$NaTcO_4$ (340 MBq ±10%). Eight participants were paired by gender and age (±1 year) with the first group and administered with the same amount of ^{99m}Tc-$NaTcO_4$ supplied commercially (eluted from generator) to serve as a control cohort. All subjects underwent a prescribed thyroid imaging procedure and an additional whole-body scan.

Safety Monitoring

The safety was assessed by monitoring vital signs, biochemical laboratory tests, and adverse events at various time points during the study. On the day of the procedure, the participants were examined by a physician. Physical examination included the lung, heart, vascular, lymph nodes, skin, and neurological assessment. The vital signs (body temperature, blood pressure, heart rate, and respiratory rate), electrocardiogram, and oxygen saturation level were monitored before and after tracer administration. Blood samples were collected for hematological and biochemical tests (complete blood count with differential, comprehensive metabolic panel) before and after tracer administration. Adverse events were monitored during the procedure and up to 24 hours after the procedure. Subjects were enrolled sequentially to make sure that there were no adverse events reported by previous participants.

Estimation of Internal Radiation Dose

The estimation of internal radiation dose to each individual patient was based on the amount of each technetium radioisotope present in radiopharmaceutical preparation at the

time of i.v. administration. The calculations were performed as described elsewhere (*7*) and the obtained values were compared with the predicted dose increase (*7*).

Image Acquisition

Thyroid images were acquired for 10 min in planar mode on an Infinia Hawkeye 4 SPECT/CT camera (GE Healthcare) equipped with a 3 mm pinhole collimator (image matrix 256 × 256). After thyroid imaging, anterior and posterior whole-body planar projections (4–5 bed positions, 3 min each) were acquired using a Discovery NM/CT 670 SPECT/CT camera (GE Healthcare) equipped with low-energy high-resolution collimators. Image matrix was 256 × 1024. For whole-body imaging, data were also acquired in lower (117 keV ±10%) and higher energy windows (170 keV ±10%) in addition to the standard 140.5 keV ±7.5% energy window.

Image Analysis – Biodistribution and Quality Evaluation

Qualitative image analysis based on visual interpretation was performed to compare the biodistribution of ^{99m}Tc-pertechnetate produced by both methods. Two nuclear medicine specialists were asked to rate the uptake as *absence*, *light uptake* or *intense uptake* in the brain, thyroid, salivary glands, heart blood pool, lungs, liver, stomach, bladder, soft tissue, and bones. Then, readers were asked to rate the biodistribution as normal or abnormal for ^{99m}Tc-pertechnetate, taking into account the presence of specific diseases which may modify the biodistribution (for example, complete thyroid resection explaining the absence of thyroid uptake, gastric hiatal hernia indicating mediastinal uptake). To evaluate image quality, both nuclear medicine specialists were shown the images randomly and were asked to tentatively discriminate between ^{99m}Tc-pertechnetate production methods.

Quantitatively, to evaluate possible interference due to scatter from high-energy isotopic impurities, the geometric mean of the raw count data from the anterior and posterior

whole-body projections in each acquisition were computed for the standard, lower, and higher energy windows. The ratios of the geometric mean counts in lower-to-standard and higher-to-standard energy windows were then calculated and compared for the cyclotron- and generator-produced radiotracers.

Statistics

Blood test results, biochemistry, and vital signs were compared before and after ^{99m}Tc-pertechnetate injection with a Wilcoxon matched-pairs signed rank test. Results with $p<0.05$ were considered significant, and clinically significant when outside of normal physiological limits.

Phantom Imaging

Planar images were acquired on the Discovery NM/CT 670 SPECT/CT camera (General Electric) equipped with low-energy high-resolution collimators (image matrix 512 × 512). Three energy windows were used for image acquisition: standard 141 keV ±7.5%, lower 120 keV ±5%, and higher 165 keV ±5%. A Jaszczak phantom (Jaszczak Flangeless Deluxe SPECT Phantom, Biodex, cold rod diameters: 4.8, 6.4, 7.9, 9.5, 11.1 and 12.7 mm; cylinder interior dimensions: ∅ 20.4 cm × 18.6 cm) filled with a solution of sodium pertechnetate ^{99m}Tc was positioned vertically on top of the camera collimator. Images (n=1 at each time point) were acquired to reach a comparable total number of counts with generator-eluted ^{99m}Tc (730 MBq) and cyclotron-produced ^{99m}Tc (620–746 MBq) at 5, 7.5, 9, 11, 13, 15, 17 h after the end of bombardment (EOB). Image contrast and contrast-to-noise ratio (*CNR*) were calculated using the following equations:

$$Contrast = \frac{R_{hot} - R_{cold}}{R_{cold}}; \quad CNR = \frac{\frac{R_{hot} - R_{cold}}{R_{cold}}}{\sqrt{(\frac{\sigma_{hot}}{R_{hot}})^2 + (\frac{\sigma_{cold}}{R_{cold}})^2}}$$

where R_i are expressed in counts per second per pixel and σ_i are standard deviations. The R_{cold} values were determined by averaging the background count rates in the largest (12.7 mm) cold spots, while the R_{hot} values were estimated in a large region-of-interest surrounding the cold spots.

RESULTS

Provision of Sodium Pertechnetate ^{99m}Tc

Cyclotron-produced ^{99m}Tc-$NaTcO_4$ solutions for injection had a radioactive concentration of 329±84 MBq/ml (range 230–471 MBq/ml), pH 5.0–5.5, radiochemical purity of at least 98%, and radioisotopic purity greater than 99.97% (Table 1). All prepared batches complied with standard requirements for parenteral injections, including sterility and endotoxin level.

Patient Demographics and Study Design

Eleven participants, administered with the cyclotron-produced ^{99m}Tc-$NaTcO_4$, received 325±29 MBq (range 271–353 MBq). The majority of subjects were female (73%). The mean age was 44.7±17.3 (19–77, median 45). The body mass index was 26.3±5.8 (range 17.2–35.8). Four out of 11 patients had Graves' disease, 4 had thyroiditis, and the others were with hypothyroidism, subclinical hyperthyroidism, or multinodular goiter. The cyclotron-produced ^{99m}Tc-pertechnetate was administered between 4 h 40 min and 7 h 3 min (280–423 min) after the EOB. On average, the time of injection was approximately 6 h from EOB.

Eight participants, paired by age and gender with the first group, were administered with the conventional ^{99m}Tc-$NaTcO_4$ and received 342±5 MBq. In this cohort, 75% of the participants were female. The mean age was 43.8±13.9 (28–66, median 41). The body

mass index was 23.8±8.0 (range 16.2–39.8). By indication, 2 had Graves' disease, 2 subclinical hyperthyroidism, 2 non-functional nodules, 1 multinodular goiter, and 1 thyroiditis. The patients were not paired by clinical indication.

All subjects enrolled in the study completed the trial. Nevertheless, 2 participants did not undergo the entire study protocol due to technical issues. One patient injected with cyclotron-produced ^{99m}Tc-$NaTcO_4$ had an incomplete blood test. Patient demographics are summarized in Table 2.

Safety Evaluation

For the cyclotron-produced ^{99m}Tc-$NaTcO_4$, the heart rate and blood pressure were within normal limits for all patients and did not change significantly before and after injection. Hematological and biochemical test results did not show any significant changes and were well set within physiological values (Table 3). No clinically detectable pharmacologic effects or adverse events were reported during the study.

Dosimetry

On average, the increase in effective dose was 1.5±0.4% when compared to ^{99m}Tc-pertechnetate without any radionuclidic impurities.

Imaging

At the time of imaging, low level radioactivity was still present in the blood pool. Low level radioactivity was also observed in the lungs, liver, bone, and soft tissues. The salivary glands, stomach, kidneys and bladder showed the highest uptake among the non-targeted organs, as expected. Tracer uptake in the thyroid varied from weak to strong and was dependent on the underlying pathology as exemplified by Fig. 1. As expected for the sodium pertechnetate ^{99m}Tc, there was no uptake in the brain. The organ distributions were the same for men and women, as can be seen in representative male and female images

(Fig. 2). Among matched subjects, the organ distribution was identical for the cyclotron-produced and generator-eluted ^{99m}Tc-pertechnetate (Fig. 3).

Visually, the images acquired in the standard and lower energy windows were equivalent for the cyclotron-produced and generator-eluted ^{99m}Tc-pertechnetate. Readers were unable to classify the images according to the origin of ^{99m}Tc because of the absence of systematic image features (inter-observer kappa value 0.17, chi-square p = 0.83). The count rate observed in the higher energy window increased considerably for the cyclotron-produced ^{99m}Tc-pertechnetate resulting in a subject's faint silhouette on an almost uniform background (Fig. 2). Since no characteristic gamma rays from contaminants can be identified in the 170 keV ± 10% range, most detected events in the higher energy window are scatters form high-energy gamma rays. The high uniform background in the higher energy window suggests the same.

Image analysis

The ratios of counts in lower-to-standard energy window were comparable for the cyclotron-produced (59±2%) and generator-eluted (54±4%) radiotracer. For the higher-to-standard energy window, the ratio was significantly higher for the cyclotron-produced ^{99m}Tc-pertechnetate (15±3% versus 4±1%), which is in accordance with the visual image interpretation (Fig. 2). Data for individual study participants are presented in Table 4. Count ratios in the higher energy window (170 keV ± 10%) are consistent with the expected buildup of longer-lived ^{96}Tc (Fig. 4).

Phantom Imaging

Phantom imaging data (Fig. 5) were in agreement with the information derived from patients' scans. We observed an increase in the ratio of counts in higher energy window from 2% with generator ^{99m}Tc to 4–10% with cyclotron-produced ^{99m}Tc and this increase

was dependent on the time elapsed after EOB (Fig. 6). Nevertheless, the contrast and contrast-to-noise ratio in the standard energy window remained stable over the course of experiment (up to 18 h after irradiation) (Fig. 6).

DISCUSSION

The main distinctive feature of cyclotron-produced ^{99m}Tc compared to generator-eluted ^{99m}Tc is the presence of other Tc isotopes (Table 1) that may contribute to additional radiation dose to patients and affect image quality. The radioisotopic purity of sodium pertechnetate ^{99m}Tc produced using a cyclotron at medium energies (E_{in} = 20–24 MeV) was previously evaluated and it was confirmed that the quality of the final formulation can be fully adequate for clinical use, provided that the isotopic composition of the starting molybdenum together with its irradiation parameters (energy, time) were appropriately selected (*7*). Although the radiochemical entity in the cyclotron-produced formulation, sodium pertechnetate ^{99m}Tc, is the same as in a generator-eluted formulation, the raw materials and chemical reagents used for its manufacturing are different. Therefore, the cyclotron-produced radiopharmaceutical formulation needed to be assessed for safety for human use, and its imaging efficacy confirmed in a clinical study with a limited number of patients.

Eleven patients were successfully imaged with cyclotron-produced sodium pertechnetate ^{99m}Tc. The injection was well tolerated and the participants did not report any discomfort due to tracer administration. Safety evaluation results did not show any alteration in the sequential blood values and vital signs.

All Tc isotopes are chemically equivalent and will have the same biological retention and distribution. For the purpose of effective dose estimation, however, the actual

residence time depends on the physical half-life of each isotope. In addition, particle emission profile and energy are different for individual isotopes. Therefore tissue/organ absorbed dose will vary for each Tc isotope. Since relative proportion of Tc isotopes in the formulation changes with time because of their distinct decay characteristics, the radioisotopic content of the product at the time of i.v. administration must be used to estimate patients' dose. The obtained values, expressed as a percent dose increase compared with ^{99m}Tc without any radionuclidic impurities (Fig. 7), fitted well with our previous calculations (*7*). The estimated effective dose increase observed in this study was minimal and well below the postulated acceptable limit of 10%. It should be noted, that ^{99m}Tc eluted from generators also contains radionuclidic impurities (*9–11*), but their contribution is not accounted for in dose assessment because biokinetic data are not available for all nuclides and/or their corresponding radioactive chemical species. Recently, another group applied a theoretical model to investigate the influence of isotopic composition of starting molybdenum on potential dose increase to patients and suggested thresholds for isotopic contamination of initial ^{100}Mo by other Mo isotopes (*12*).

As expected, the whole body images confirmed normal distribution of the ^{99m}Tc-pertechnetate in thyroid, salivary glands, stomach, and urinary bladder. This was also exemplified through comparative assessment of images taken of paired participants (Figs. 2 and 3). Images of the thyroid also correlated well with the underlying pathology (Fig. 1, Table 2), which provides supporting evidence of the suitability of the cyclotron-produced ^{99m}Tc-pertechnetate for diagnostic clinical use.

No particular characteristics were underlined by the two nuclear medicine specialists when asked to find which patients were injected with cyclotron-produced pertechnetate. Clinically, images were of similar quality and biodistribution. Impurities present in the

cyclotron formulation did not create any clinically relevant features in the images obtained in the standard energy window.

Quantitatively, for the cyclotron-produced ^{99m}Tc, the ratio of counts increased by approximately 9% in the lower energy window (from 54±4% to 59±2%). At the same time, a 4-fold increase (from 4±1% to 15±3%) was observed in the higher energy window (Table 4). Nonetheless, despite the increased background in adjacent energy windows, trace amounts of isotopic impurities present in the cyclotron-produced ^{99m}Tc did not affect in any significant way the image definition in the standard energy window. As demonstrated with phantoms earlier (*7*) and in this work (Figs. 5 and 6), the spatial resolution and contrast in the standard energy window remained comparable for both cyclotron-produced and generator-eluted ^{99m}Tc. Theoretical simulations support these findings (*13*). Therefore, the effect that may be due to scattering of high energy gamma-rays originating from isotopic contaminants such as ^{94}Tc, ^{94m}Tc, and ^{96}Tc, can be considered negligible as long as the product meets radionuclidic purity specifications based on dosimetry considerations or product shelf-life, whichever is shorter.

Production of ^{99m}Tc with cyclotron is a reiterated idea (*14*) that received little attention before the supply of inexpensive and readily available ^{99m}Tc from ^{99}Mo generators became fragile. In recent years, several groups, including our consortium, developed new targets and robust separation procedures to manufacture high-purity ^{99m}Tc with cyclotrons (*7*, *15–20*). There is increasingly convincing evidence that the quality of cyclotron-produced ^{99m}Tc is comparable to the conventional ^{99m}Tc (*7*, *21–24*) and that sufficient quantities can be made to satisfy the demand of large urban communities (*3*). This clinical trial confirmed that cyclotron-produced sodium pertechnetate ^{99m}Tc provides equivalent clinical safety and diagnostic efficacy as the conventional radiopharmaceutical. Now, whether the cyclotron-

produced ^{99m}Tc will reach the status of an approved radiopharmaceutical or be forgotten again remains to be seen. While the cost of its commercialization (infrastructure, marketing authorization) may be orders of magnitude lower than nuclear reactor-based production, it is still significant and will require commitment from governments and investors. Economic factors, including implementation of full-cost recovery models for ^{99}Mo/^{99m}Tc production (*2*), will be a decisive point in this almost half-a-century old story.

CONCLUSION

We showed that ^{99m}Tc produced using a cyclotron at medium energy can be safely used for humans and yields clinical images that are fully satisfactory for diagnostic procedures. The results of this work provide further supporting evidence for the adoption of cyclotron-produced sodium pertechnetate in clinical practice.

DISCLOSURE

This work was supported by Natural Resources Canada through the Isotope Technology Acceleration Program (ITAP) and by Medical Imaging Trial Network of Canada (MITNEC). The Research Center of CHUS (CRCHUS) is supported by the Fonds de recherche du Québec – Santé (FRQS).

ACKNOWLEDGEMENTS

The authors gratefully acknowledge Jim Garrett from the Laboratory of Materials Preparation and Characterization of the Brockhouse Institute for Materials Research, McMaster University, for preparing ^{100}Mo targets. We thank cyclotron operators, Eric Berthelette and Paul Thibault, for their excellent technical help and continuing availability

for this research project, and Otman Sarrhini for phantom image analysis. We acknowledge our ITAP partners, University of Alberta and Advanced Cyclotron Systems Inc.

REFERENCES

1. Rahmim A, Zaidi H. PET versus SPECT: strengths, limitations and challenges. *Nucl Med Comm*. 2008;29:193–207.
2. Organization for Economic Co-operation and Development, Nuclear Energy Agency. Full-cost recovery for molybdenum-99 irradiation services: methodology and implementation. Guidance document NEA/SEN/HLGMR(2012)9. http://www.oecd-nea.org/med-radio/guidance/docs/full-cost-recovery-molybdenum-99-irradiation.pdf
3. Bénard F, Buckley KR, Ruth TJ, et al. Implementation of multi-Curie production of ^{99m}Tc by conventional medical cyclotrons. *J Nucl Med*. 2014;55:1017–1022.
4. McEwan A, McQuarrie S, Abrams D, et al. Technetium-99m (Tc-99m) pertechnetate (TcO_4) imaging with cyclotron produced Tc-99m compared with generator Tc-99m. [abstract] *J Nucl Med*. 2012;53(Suppl.1):1487.
5. Celler A, Hou X, Bénard F, Ruth T. Theoretical modeling of yields for proton induced reactions on natural and enriched molybdenum targets. *Phys Med Biol*. 2011;56:5469–5484.
6. Lebeda O, van Lier EJ, Štursa J, Ráliš J, Zyuzin A. Assessment of radionuclidic impurities in cyclotron produced ^{99m}Tc. *Nucl Med Biol*. 2012;39:1286–1291.
7. Selivanova SV, Lavallée É, Senta H, et al. Radioisotopic purity of sodium pertechnetate ^{99m}Tc produced with a medium-energy cyclotron: implications for internal radiation dose, image quality, and release specifications. *J Nucl Med*. 2015;56:1600–1608.
8. McAlister DR, Horwitz EP. Automated two column generator systems for medical radionuclides. *Appl Radiat Isot*. 2009;67:1985–1991.
9. Council of Europe, European pharmacopeia, Monograph 124, Sodium pertechnetate (^{99m}Tc) injection (fission), 2005.

10. Council of Europe, European pharmacopeia, Monograph 283, Sodium pertechnetate (^{99m}Tc) injection (non-fission), 2005.

11. United States Pharmacopeial Convention, Official Monographs: USP32–NF27, Sodium Pertechnetate Tc 99m Injection, 2010.

12. Hou X, Tanguay J, Buckley K, et al. Molybdenum target specifications for cyclotron production of ^{99m}Tc based on patient dose estimates. *Phys Med Biol*. 2016;61:542–553.

13. Hou X, Tanguay J, Benard F, et al. Investigation of the impact on image resolution of trace impurities found in cyclotron-produced Tc pertechnetate. [abstract] *J Nucl Med*. 2015;56(Suppl.3):1749.

14. Beaver JE, Hupf H. Production of 99mTc on a medical cyclotron: a feasibility study. *J Nucl Med*. 1971;12:739–741.

15. Targholizadeh H, Raisali G, Jalilian AR, Rostampour N, Ensaf M, Dehghan MK. Cyclotron production of technetium radionuclides using a natural metallic molybdenum thick target and consequent preparation of [Tc]-BRIDA as a radio-labelled kit sample. *Nukleonika*. 2010;55:113−118.

16. Morley TJ, Dodd M, Gagnon K, et al. An automated module for the separation and purification of cyclotron-produced $^{99m}TcO_4^-$. *Nucl Med Biol*. 2012;39:551–559.

17. Gagnon K, Wilson JS, Holt CMB, et al. Cyclotron production of ^{99m}Tc: Recycling of enriched ^{100}Mo metal targets. *Appl Radiat Isot*. 2012;70:1685–1690.

18. Andersson J, Wilson J, Thomas B, et al. Tentagel as chromatography media for processing cyclotron produced ^{99m}Tc. [abstract] *J Nucl Med*. 2014;55(Suppl.1):1248.

19. Hanemaayer V, Benard F, Buckley KR, et al. Solid targets for ^{99m}Tc production on medical cyclotrons. *J Radioanal Nucl Chem*. 2014;299:1007–1011.

20. Bénard F, Zeisler SK, Vuckovic M, et al. Cross-linked polyethylene glycol beads to separate ^{99m}Tc-pertechnetate from low-specific-activity molybdenum. *J Nucl Med*. 2014;55:1910–1914.

21. Guérin B, Tremblay S, Rodrigue S, et al. Cyclotron production of ^{99m}Tc: An approach to the medical isotope crisis. *J Nucl Med*. 2010;51:13N–16N.

22. Lebeda O, van Lier EJ, Štursa J, Ráliš J, Zyuzin A. Assessment of radionuclidic impurities in cyclotron produced ^{99m}Tc. *Nucl Med Biol*. 2012;39:1286–1291.

23. Rovais MRA, Aardaneh K, Aslani G, Rahiminejad A, Yousefi K, Boulouri F. Assessment of the direct cyclotron production of ^{99m}Tc: An approach to crisis management of ^{99m}Tc shortage. *Appl Radiat Isot*. 2016;112:55–61.

24. Das MK, Madhusmita, Chattopadhyay S, et al. Production and separation of ^{99m}Tc from cyclotron irradiated $^{100/natural}$Mo targets: a new automated module for separation of ^{99m}Tc from molybdenum targets. *J Radioanal Nucl Chem*. 2016; DOI 10.1007/s10967-016-4796-3.

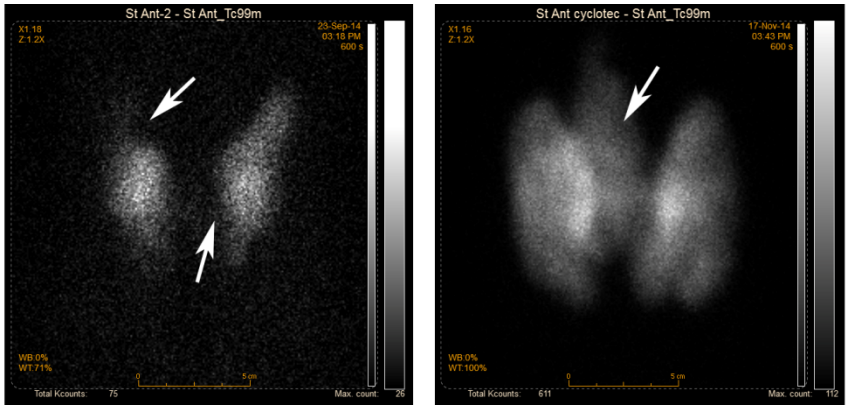

FIGURE 1. Examples of thyroid images produced with the cyclotron-produced sodium pertechnetate ^{99m}Tc. *Left:* Low radioactivity accumulation in cold nodules (arrows) in the upper inner right lobe and in the isthmus in proximity of the left lobe of the thyroid gland. *Right:* High accumulation in the thyroid gland with a visible pyramidal lobe (arrow) in case of hyperthyroidism (Graves' disease).

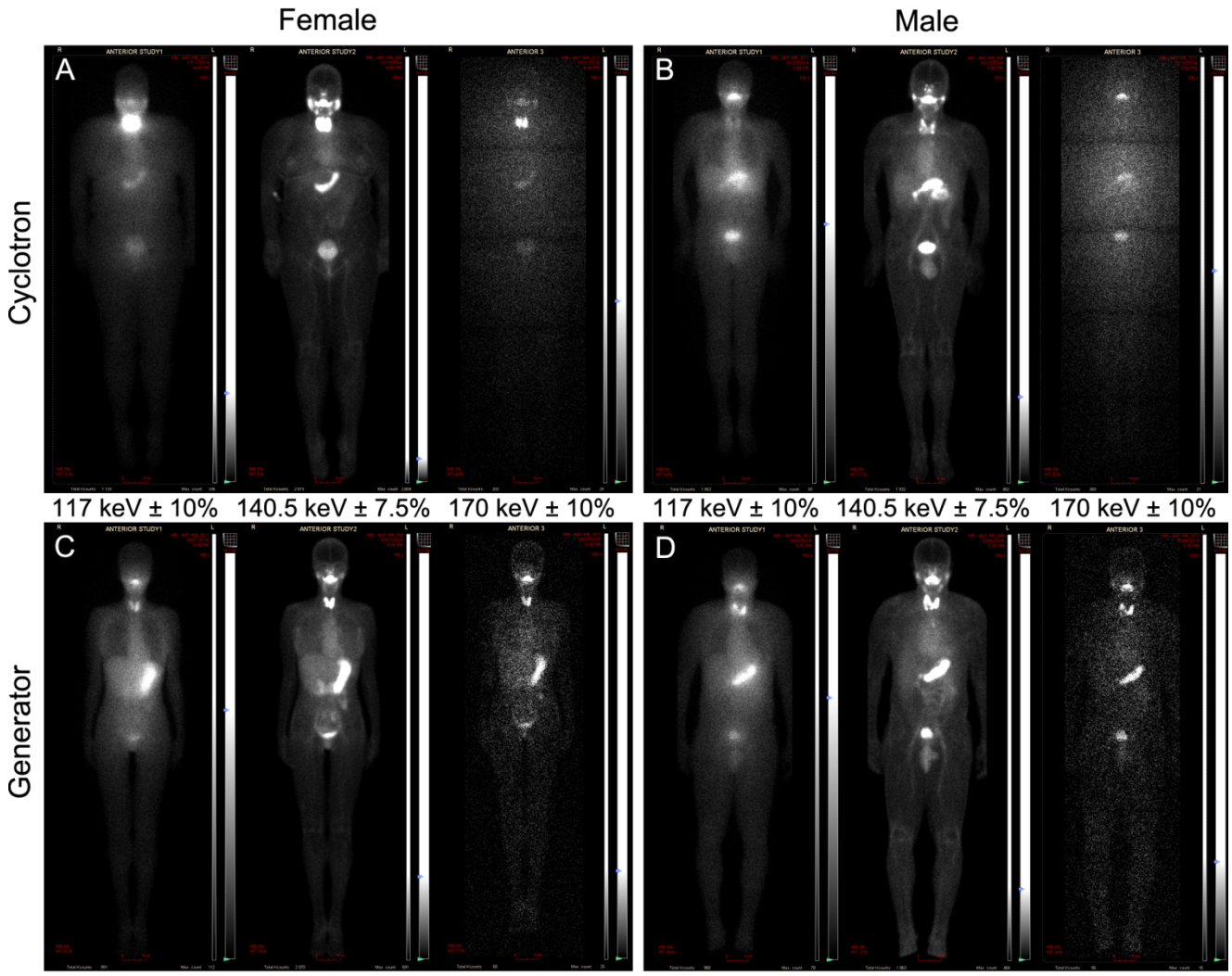

FIGURE 2. Two female and two male participants scanned with cyclotron-produced (A: patient C2, B: patient C6) or generator-eluted (C: patient G6, D: patient G7) sodium pertechnetate ^{99m}Tc; anterior images are shown. Visually, the image quality is identical in the standard (*middle* in each quadrant) and lower (*left* in each quadrant) energy windows. Increased uniform background was observed in the higher (*right* in each quadrant) energy window for the cyclotron-produced ^{99m}Tc. (See Table 2 for patient data.)

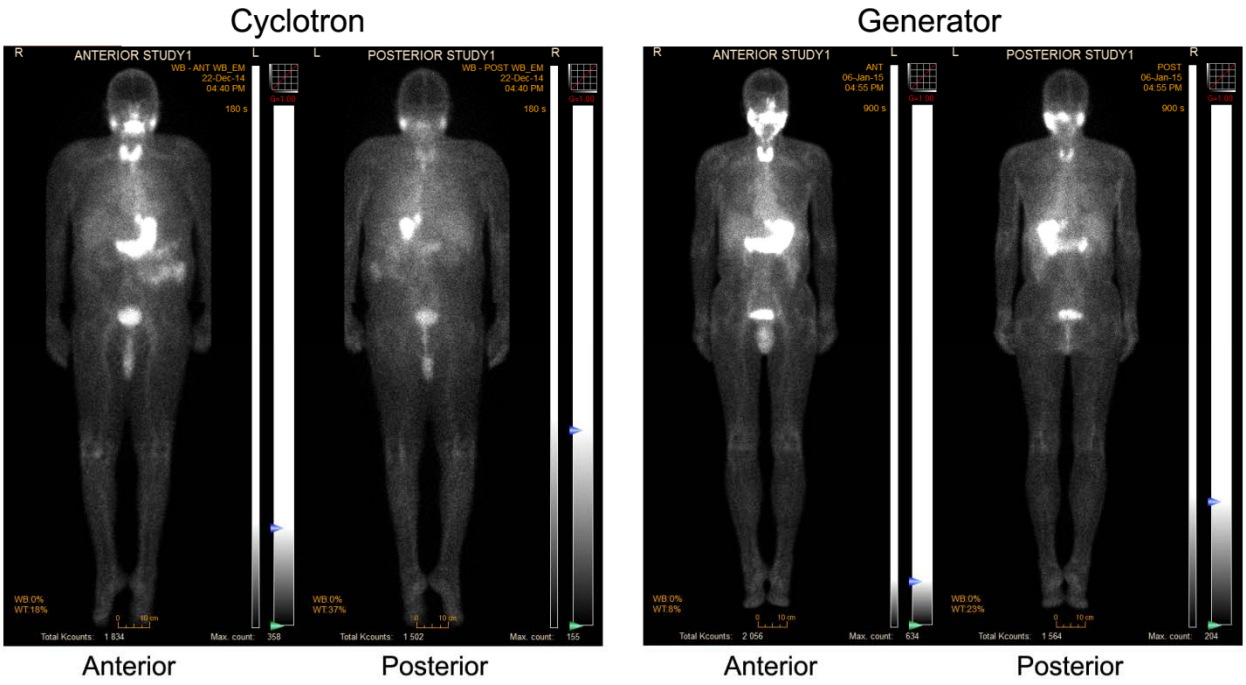

FIGURE 3. Two male patients, both with thyroiditis, scanned with cyclotron-produced (*left*, patient C8) or generator-eluted (*right*, patient G2) sodium pertechnetate ^{99m}Tc. Images acquired in the standard energy window are visually equivalent in terms of expected biodistribution of the tracer as well as image quality.

FIGURE 4. Count ratios of higher to standard energy windows increase steadily with the expected buildup of longer-lived ^{96}Tc.

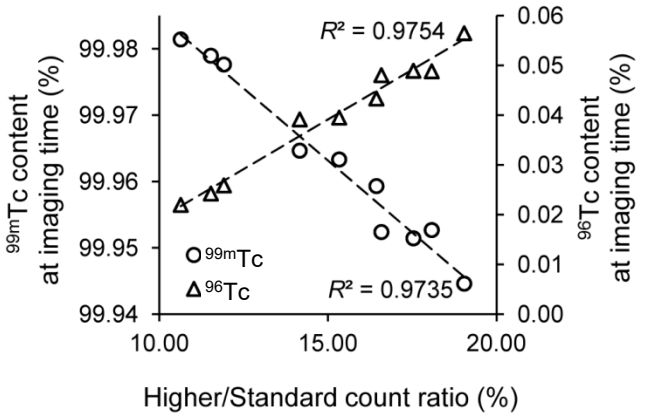

FIGURE 5. Typical phantom images obtained with cyclotron-produced (*top*, 723 MBq, 9 h after EOB) and generator-eluted ^{99m}Tc (*bottom*, 730 MBq). Images are on a linear grey scale with white being the maximum intensity. Cold rods are 4.8, 6.4, 7.9, 9.5, 11.1, and 12.7 mm in diameter.

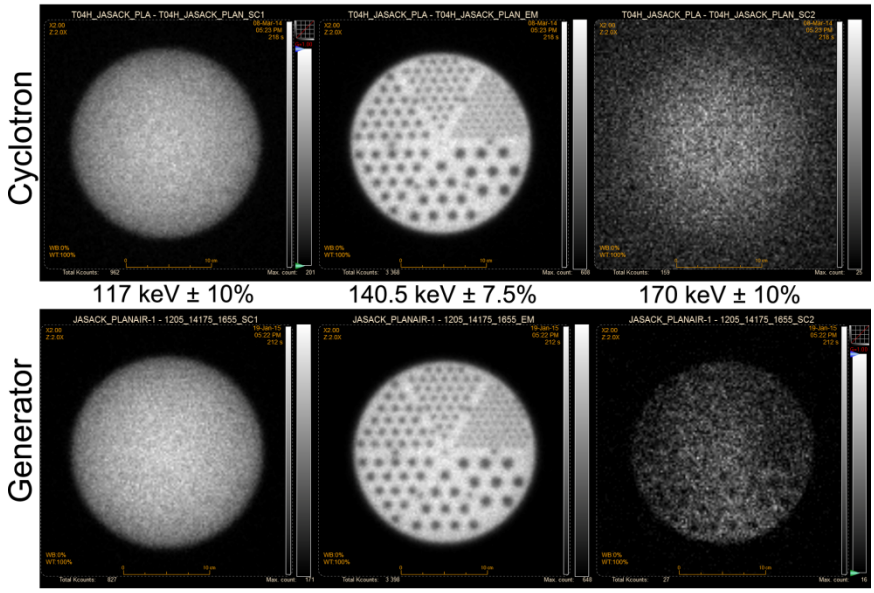

FIGURE 6. Left: Ratio of counts in lower and higher energy windows to those in standard energy window as a function of time. Right: Contrast and contrast-to-noise ratio in the standard energy window as a function of time.

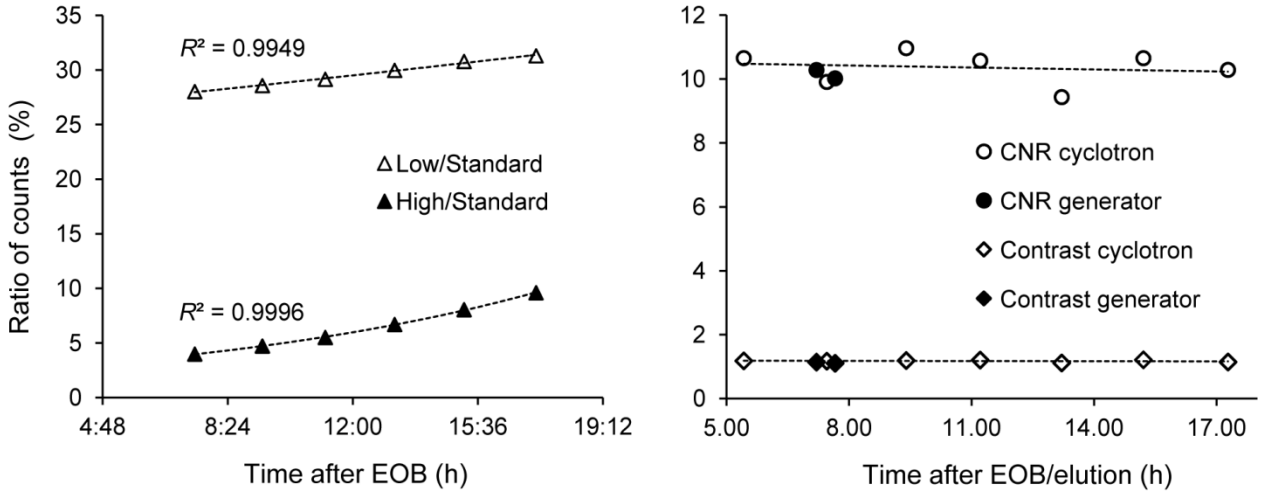

FIGURE 7. Estimated equivalent effective dose increase for each patient injected with the cyclotron-produced ^{99m}Tc. Solid line: predicted radiation dose increase (*7*).

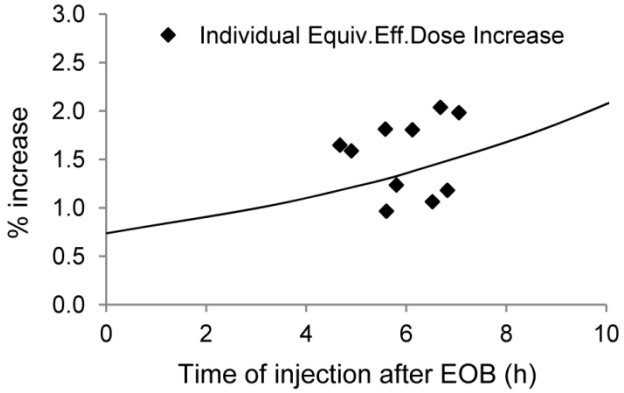

TABLE 1. Radioisotopic composition of the cyclotron-produced (24→19±1 MeV, 2 h) sodium pertechnetate ^{99m}Tc at EOB.

Nuclide[#]	**Half-life** $T_{1/2}$ **(h)**	**Gamma-ray energy** E_γ **(keV)**	**Content**[##] **(%)**
^{99m}Tc	6.015	140.511	99.979±0.009
^{97m}Tc	2184	96.5	0.0006±0.0001
^{96}Tc	102.7	812.54	0.013±0.007
^{95}Tc	20	765.789	0.0017±0.0003
^{95m}Tc	1464	582.082	0.000008±0.000005
^{94}Tc	4.9	702.67	0.0023±0.0004
^{93}Tc	2.75	1362.94	0.0032±0.0004

[#]Physical properties are from the Brookhaven National Laboratory National Nuclear Data Center, Nuclear structure and decay data NuDat 2.5 (2011), http://www.nndc.bnl.gov/nudat2

[##] Measured by γ-ray spectrometry (*7*)

TABLE 2. Demographic data.

	Participant	Gender	Indication	Age (years)	Body-Mass Index	Administered activity (MBq)	Injection time (hours after EOB)	Imaging time (whole-body) (hours after EOB)	Estimated effective dose increase (%)	Imaging findings according to indication
CYCLOTRON	C1	F	Bilateral thyroid nodule	45	28.0	296.8	5:03	6:34	–	Hypothyroidism
	C2	F	Hyperthyroidism, Graves' disease	49	31.3	351.5	6:31	7:29	1.04	Graves' disease
	C3	F	Multinodular goiter	77	25.0	291.4	5:48	7:32	1.20	Subclinical hyperthyroidism
	C4	F	Hypothyroidism	34	19.4	351.0	5:36	6:34	0.94	Thyroiditis
	C5	F	Hyperthyroidism	28	17.2	353.3	6:49	7:52	1.15	Thyroiditis, goiter?
	C6	M	Nodules	60	22.7	329.9	4:54	6:13	1.54	Multinodular goiter
	C7	F	Graves disease	19	25.5	270.7	6:07	7:04	1.75	Graves' disease
	C8	M	Hyperthyroidism de novo	65	27.6	330.2	4:40	6:03	1.60	Thyroiditis
	C9	F	Hyperthyroidism	47	35.8	308.6	6:41	7:32	1.98	Graves' disease
	C10	F	Thyroiditis or hyperthyroidism	32	34.1	347.7	5:35	6:13	1.76	Thyroiditis
	C11	M	Hyperthyroidism	36	22.6	348.4	7:03	9:00	1.93	Graves' disease
GENERATOR	G1	F	Nodule	34	39.8	345.6	NA	NA	NA	Non-functional nodular formation
	G2	H	Hyperthyroidism	66	21.1	346.5	NA	NA	NA	Thyroiditis
	G3	F	Goiter, Graves' disease	31	24.2	341.7	NA	NA	NA	Subclinical hyperthyroidism, suspected thyroid nodule
	G4	F	Nodules	47	19.7	340.0	NA	NA	NA	Subclinical hyperthyroidism, hyper-functional nodules
	G5	F	Hyperthyroidism	28	18.3	349.5	NA	NA	NA	Graves' disease
	G6	F	Nodules	50	16.2	334.6	NA	NA	NA	Multinodular goiter
	G7	H	Nodule	59	27.2	345.1	NA	NA	NA	Non-functional thyroid nodule
	G8	F	Hyperthyroidism	35	35.3	336.0	NA	NA	NA	Graves' disease, suspected non-functional nodule

TABLE 3. Results of the selected biochemical and hematological tests.

Analysis	Normal values	Before injection	After injection
Alanine aminotransferase	M: 0–55 IU/L F: 0–37 IU/L	27 ± 16 (n=3) 23 ± 11 (n=7)	24 ± 17 (n=3) 23 ± 11 (n=7)
Albumin	35–52 g/L	38 ± 2 (n=10)	42 ± 2 (n=10)
Aspartate aminotransferase	M: 0–40 IU/L F: 0–32 IU/L	21 ± 8 22 ± 5	19 ± 7 21 ± 6
Bilirubin (total)	2.8–17.0 µmol/L	8.5 ± 6.3	9.4 ± 7.6
Calcium (blood)	2.07–2.55 mmol/L	2.30 ± 0.07	2.27 ± 0.10
Carbon Dioxide	23.0–27.0 mmol/L	25.5 ± 2.6	25.6 ± 2.5
Chlorides (blood)	96–106 mmol/L	102 ± 3	103 ± 2
Creatinine (blood)	M: 58–110 µmol/L F: 46–92 µmol/L	80 ± 27 57 ± 10	76 ± 22 56 ± 10
Gamma-glutamyl-transferase (serum)	M: 0–64 IU/L F: 0–55 IU/L	32 ± 5 34 ± 21	33 ± 7 33 ± 21
Glucose (blood)	3.3–6.1 µmol/L	5.9 ± 1.4	5.4 ± 1.8
Lactate dehydrogenase	M: 0–250 IU/L F: 0–235 IU/L	158 ± 13 154 ± 34	133 ± 13 158 ± 30
Alkaline Phosphatase	M: 40–130 IU/L F: 35–105 IU/L	83 ± 33 72 ± 30	82 ± 32 72 ± 30
Potassium (blood)	3.5–5.1 µmol/L	4.0 ± 0.3	4.2 ± 0.3
Total Proteins (blood)	58–80 g/L	69 ± 3	68 ± 3
Sodium (blood)	135–145 µmol/L	140 ± 1	141 ± 2
Urea (blood)	M: 3.2–7.6 mmol/L F: 2.5–6.6 µmol/L	6.1 ± 0.8 3.9 ± 1.5	6.0 ± 0.8 3.6 ± 1.5
White blood cells	1 - 50 $\times 10^9$/L	7 ± 1	7 ± 2
Hemoglobin	M: 130–180 g/L F: 120–160 g/L	157 ± 13 132 ± 8	155 ± 13 132 ± 7
Platelets	20–1000 $\times 10^9$/L	235 ± 69	218 ± 74
Cholesterol	M: 2.81–4.89 mmol/L F: 2.69–5.88 mmol/L	3.81 ± 0.38 4.40 ± 0.64	3.79 ± 0.45 4.41 ± 0.71
Triglycerides	< 1.7 mmol/L	1.6 ± 1.1	1.5 ± 1.0

TABLE 4. Ratio of counts acquired in lower and higher energy windows to those in standard energy window from individual patients' images.

		Anterior-posterior geometric mean ratio	
	Participant	Lower/ Standard	Higher/ Standard
Cyclotron	C1	58 %	18 %
	C2	59 %	11 %
	C3	56 %	13 %
	C4	60 %	10 %
	C5	55 %	11 %
	C6	57 %	15 %
	C7	59 %	16 %
	C8	59 %	16 %
	C9	63 %	18 %
	C10	62 %	17 %
	C11	58 %	17 %
Generator	G1	59 %	3 %
	G2	51 %	5 %
	G3	56 %	6 %
	G4	54 %	3 %
	G5	53 %	3 %
	G6	51 %	3 %
	G7	55 %	3 %
	G8	57 %	4 %